LOW-DIMENSIONAL GALERKIN MODEL OF A PLANE MIXING LAYER-WAKE INTERACTION

Caroline Braud, Dominique Heitz, Georges Arroyo
Cemagref,
17, avenue de Cucillé,
F35044 Rennes cedex - France
caroline.braud@cemagref.fr,
dominique.heitz@cemagref.fr,
georges.arroyo@cemagref.fr

Joel Delville, Jean Paul Bonnet
L.E.A. (Laboratoire d'Etudes Aérodynamiques)
UMR CNRS 6609,
CEAT 43 Route de l'Aérodrome,
F 86036 Poitiers - France
joel.delville@lea.univ-poitiers.fr
jean-paul.bonnet@lea.univ-poitiers.fr

ABSTRACT

The complex $3D$ dynamical behavior resulting from the interaction between a plane mixing layer and the wake of a cylinder is investigated using the proper orthogonal decomposition, applied to data from two synchronized 2D PIV systems. An analysis of the correlations shows different length scales in the regions dominated by wake like structures and shear layer type structures. In order to characterize the particular organization in the plane of symmetry, a Galerkin projection from a slice POD is performed. This leads to a low-dimensional dynamical system that allows the analysis of the relationship between the dominant frequencies and leads to a reconstruction of the dominant periodic motion suspected from previous studies (Heitz, 1999).

INTRODUCTION

The interaction between a plane mixing layer and the wake of a slender body is of great interest as it occurs in practical configurations such as heat exchangers, off-shore structures, wind-turbines, smoke-stacks, etc. The motivation of the present study is directly related to air flow control problems in the food industry.

The interaction of the wake of a circular cylinder and a turbulent plane mixing layer belongs to a family of complex flows. This kind of flow as received little attention in the experimental literature. This is partly due to the highly three-dimensional flow in the near wake where experimental and numerical investigations are difficult to carry out. Nevertheless attempts have been made to understand the physical nature of the coupling between the two-dimensional and three-dimensional processes in the wake of a nominally two-dimensional cylinder. See Williamson (1996) and Bearman (1998) for reviews of the flow around circular cylinders and bluff bodies.

Flow three-dimensionalities caused by velocity shear, diameter taper, local discontinuity in cylinder diameter and end conditions are similar in behavior. In all of these flows, there is a spanwise variation of the Strouhal frequency that is tied in with the three-dimensional vorticity dynamics. For small perturbations, cells of constant frequency shedding appear. Between these regions, the neighboring vortices are forced to find suitable terminations linkages. Previous studies of this flow showed that strong interactions take place just behind the shedding body (Heitz, 1999). In the near wake, a non-stationary secondary flow from the low to the high velocity side of the shear layer was observed. The aforementioned experiments indicated that a level of organization exists in the near-wake zone of interaction. Our motivation is to describe the dynamic of the coherent structures in the mixing layer-wake region. In this context the Proper Orthogonal Decomposition is a very useful technique to extract the spatial organization of the flow and energetically dominant modes. This decomposition has been widely used in various applications like data compression and mathematical models ... see Holmes *et al.* (1996). Examples for fully inhomogeneous turbulent flows can be found in Manhart (1998); Alfonsi *et al.* (2003) who have applied POD behind a mounted cube. Recently POD has been applied to Particle Image Velocimetry (PIV) measurements (Bernero & Fiedler, 2000; Stephen *et al.*, 1999). This data type is strongly limited in time by the actual frame rates of the CCD cameras typically used for PIV. Recently, Kaehler (2000) has performed a multiple stereo PIV (dual-plane PIV) to yield a better spatio-temporal resolution. All of POD applications cited above, show that it is possible to retrieve the coherent

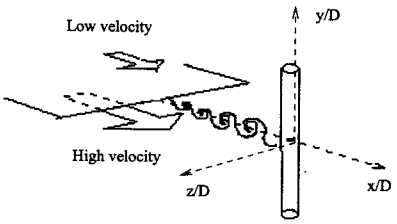

Figure 1: Flow configuration

structures observed in experiments. The POD can then be used in truncated form to produce a Low-Order Dynamical model of the flow (LOD). Ruelle & Takens (1971) proved with a theoretical approach that a few degrees of freedom is enough to get a chaotic dynamic system Holmes *et al.* (1997) showed that an attractor representation in the phase space exists if there is an exponential decay of the empirical eigenvalues extracted from POD analysis. Hence, most of the POD studies are followed by a Galerkin projection, which is a projection of the Naviers-Stokes equation onto the orthogonal basis of the POD (Aubry *et al.*, 1988; Ukeiley *et al.*, 2001; Ma & Karniadakis, 2002). In this way, a partial differential equation is reduced to an ordinary differential equation which can be analyzed with stability theory.

The goal of the present paper is to investigate the dynamics of the complex three-dimensional flow, *inhomogeneous in all three directions*, obtained by the interaction of a plane mixing layer and a wake (Fig.1). We used the classical POD, introduced by Lumley (1967), which gives a characterization of the mean organization in the near mixing layer-wake interaction area. Therefore, a two 2D PIV planes technique, hereafter called **bi-PIV**, is used to acquire a large set of data needed for our POD approach. Following from this, a Galerkin projection is used to analyze the dynamics in the wake plane of symmetry ($z = 0$). In the first section of this paper, we introduce the process of data acquisition. Then we study the mean velocities and two points correlations. In the next section, we extract eigenvectors and eigenvalues from a slice in the wake plane of symmetry. Following this, the formulation of the POD-Galerkin from this slice POD is presented. Finally, we show the results from this projection and give some interpretations.

EXPERIMENTAL DETAILS AND EXTRACTION OF POD MODES

Flow configuration

Experiments were performed in the *R300* closed-loop wind tunnel of the **CEAT** (**C**entre d'**E**tudes **A**érodynamiques et **T**hermiques). For more details about the facility, see Heitz (1999). The velocity ratio between the two streams was r=U_b/U_a=0.65, with an average convective velocity U_m=$(U_a + U_b)/2$=14.85 m/s (U_b=11.7 m/s and U_a=18 m/s) giving an average Reynolds number, based at the cylinder diameter $D = 8mm$, of 7920. Preliminary hot-wire measurements have shown that without the cylinder, the plane mixing layer reaches the self-similarity state at a downstream distance of 140 mm from the trailing edge of the splitter plate. The expansion factor $\sigma = \sqrt{\pi}(d\delta_\omega/dx)^{-1}$ is found to be about 48. The circular cylinder is placed so that its diameter corresponds to the local vorticity thickness at the cylinder location, δ_{ω_o}=D=8 mm. The coordinate system is x in streamwise direction, y in cross-stream (vertical, parallel to the axis of the cylinder) and z in spanwise direction (parallel to the plate). The high velocity is on the bottom side (y negative) and low velocity on the upper side (y positive) of the splitter plate. The origin is taken so that x=0 and z=0 on the cylinder axis and y=0 on the centerline of the trailing edge of the splitter plate (Fig.1). The z=0 plane represents the plane of symmetry that will be used for development of the dynamical system.

Experiments

In order to generate the 3D-two components velocity correlation tensor, making it possible to use a "classical POD", two parallel PIV planes are arranged perpendicularly to the splitter plate ($x - y$ planes) (Fig. 2). Measurements were performed for a set of spanwise separations between the PIV-planes (over a mesh of 21 planes locations). The extent of the measurement domain is $L_x \times L_y \times L_z = 10.5 \times 7.75 \times 8\ .D^3$. This area is limited to the near downstream zone of the cylinder. Due to the inhomogeneity in the all three spatial directions, every combination of the two planes over this mesh has to be considered, leading to a set of 231 configurations.

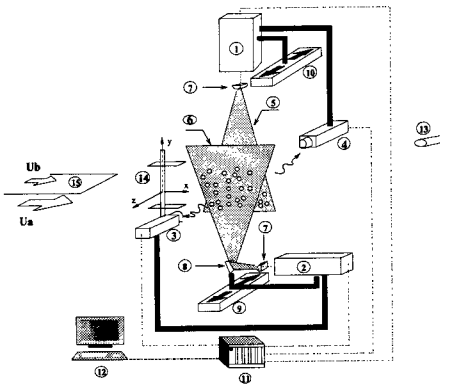

Figure 2: Set-up of the "bi-PIV" experiments

The PIV setup is described in Figure 2. Each of the camera-lasers couple (2,3) and (1,4) is jointly displaced parallel to the z axis (9,10), to keep the focal adjustment. In order to separate the two PIV planes, created by NdYag lasers (30 mJ per pulse, QUANTEL and NEWWAVE (1,2)), polarizing filters are used. Acquisition and synchronization was performed with a DANTEC *FLOWMAP processor* (12). Images were grabbed by two CCD cameras (KODAK type 700, 768 × 486 pixels, 8 bits (3,4)). The flow was seeded with olive oil tracer particles.

Finally, a full 3D correlation tensor was calculated, for $p, q = 1, ..., Nz$, where N_z is the number of spanwise positions:

$$R_{ij}(\mathbf{x}, \mathbf{x}') = \left[R_{ij}(x, y, z_p, x', y', z'_q)\right] \quad (1)$$

More details about how the 3D correlation tensor has been evaluated and can be found in Braud *et al.* (2002).

Mean Flow

The main topological characteristics found from this PIV experiment are very close to that found in previous results by other experimental means (Heitz, 1999). The global behavior of this particular flow can be observed from the mean velocity profiles, plotted in Fig. 3 in a $z - y$ plane at $x = x_a = 5.53D$ (center of the domain extent in the x direction). From the streamwise mean velocity profiles U, one can observe the footprint of the mixing layer and of the wake for $|z/D| \sim 4$ and for $|y/D| \sim 3$ respectively, while for smaller values of z and y, the wake-mixing layer interaction zone shows that the velocity deficit corresponding to the high velocity side is of the order of magnitude of ΔU=$U_a - U_b$ (Fig. 3a). In this region, a strong global flow motion towards the high velocity side can be observed. For $|z/D| < 1$, the vertical velocity mean component V is of the order of $20\%\Delta U$, on the high velocity side (Fig. 3b). This

strong motion can also be observed in the symmetry plane, $z = 0$, close to the cylinder where V is of the order or ΔU (Fig. 4c).

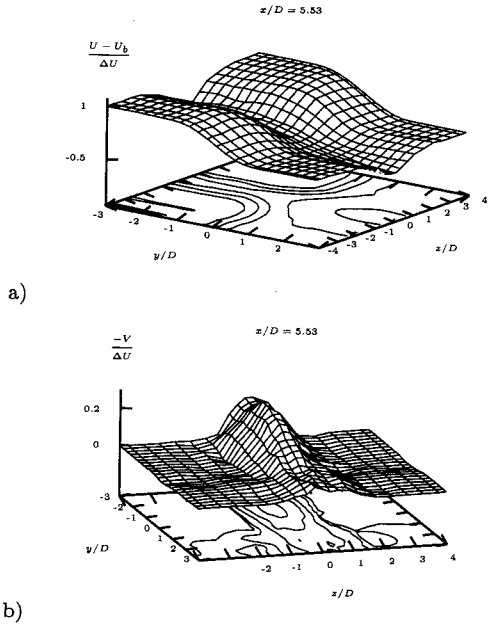

Figure 3: Mean velocity components in the streamwise plane ($x = 5.53D$): a) $\frac{U-Ub}{\Delta U}$ b) $\frac{-V}{\Delta U}$

The streamwise evolution of the mean flow is illustrated in figure 4 where velocities are plotted in $x - y$ planes. In the plane far from the cylinder influence, $z/D = 3D - 4$ (Fig. 4a), the mean streamwise velocity U profiles exhibit a typical mixing layer evolution, with a linear growth and an expansion factor of $\sigma = 47.8$ close to that found in the mixing layer without the circular cylinder ($\sigma = 48$). In the symmetry plane $z/D = 0$ these profiles are representative of the length of the recirculating zone behind the cylinder (Fig. 4b). This length is greater on the high velocity side than on the low velocity side, with a contraction of the isocontours in the mixing layer area.

Two point correlations

The first step in the analysis of the organization of this flow configuration involves the examination of the velocity correlations. Figure 5 shows such correlations obtained for the streamwise fluctuating velocity component, u, in various $x - y$ planes, with $z = z'$. Correlations are shown for the planes that correspond to the *mixing layer like behaviour* zone ($z/D = 4$) (a), the wake-shear area ($z/D \sim 0.9$) (b) and the cylinder axis ($z/D = 0$) (c). In these plots, the reference point $\mathbf{A} = (x_a, y_a)$ is located at the center of the investigation domain. Position $\mathbf{A}$ corresponds to the intersection of the drawn horizontal and vertical lines, $x/D = 5.5$, $y/D = 0$. For each plot in figure 5 a set of 10 isocontours are shown for the positive and negative correlation values. They are equally distributed between the minimum negative and maximum positive level respectively. As can be observed in this figure, the correlations change greatly in shape and integral length scales, depending on the spanwise location of the $x - y$ plane. Integral streamwise length scales Λ_x can be extracted from these plots, provided by the distance between the centers of the negative isocontours zones surrounding the positive correlation area near the reference point. These

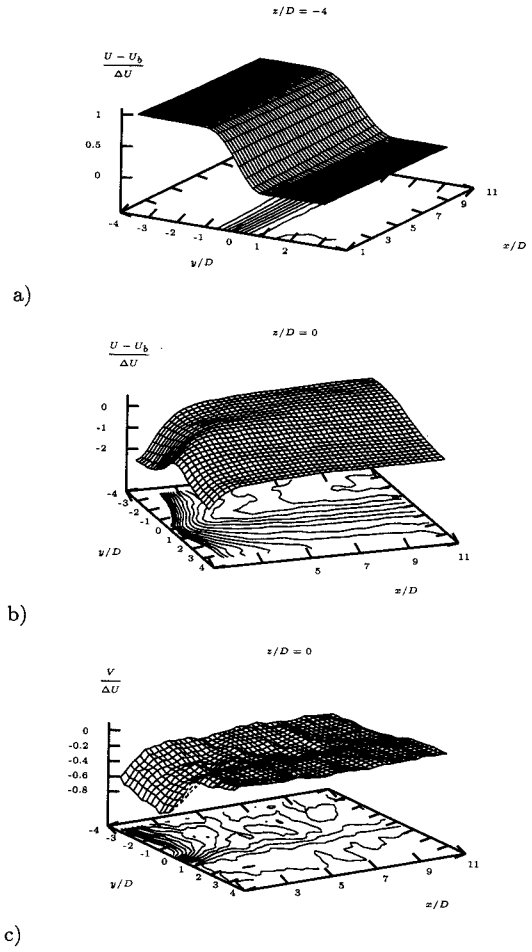

Figure 4: Mean velocity : a)Spanwise plane ($z = -4D$) $\frac{U-Ub}{\Delta=U}$; plane of symmetry($z/D = 0$) : b) $\frac{U-Ub}{\Delta U}$ c) $\frac{V}{\Delta U}$

scales can be compared to conventional Strouhal numbers, through a Taylor hypothesis: $S_t = f_p \mathcal{D}/U_m = \mathcal{D}/\Lambda_x$ where f_p is the typical *structure passing frequency* and $\mathcal{D}$ is a *local size of the structures eg. the vorticity thickness* δ_ω. In the mixing layer flow, $z/D = -4$, Fig. 5a), using $\delta_{\omega_a} \simeq$11.5mm at $x = x_a$, S_t is found to be 0.22 and is in good agreement with its conventional value measured on a mixing layer axis (Delville *et al.*, 1999). An equivalent passing frequency can then be defined $f_{p_a} \sim$ 300Hz.

In the wake-shear area ($z/D = -0.9$), the streamwise correlations exhibit a high level of spatial organization (Fig. 5b). This organization is distinct for each side of the mixing layer axis. On the high velocity side, a strong slant appears in the correlation function, which begins at the splitter plate level, $y/D = 0$. The Strouhal number, $S_t = 0.22$, on the high speed side is close to that which was was found in the mixing layer region.

This result confirms the organization pattern discussed in Braud *et al.* (2002). It has been related to the mixing layer, which gives rise to the simultaneous presence of two types of cell arrangement, with two different frequencies. This results in the propagation of an oblique shedding mode on both sides of the wake, i.e. the high velocity and low velocity side of the wake. Furthermore, this oblique shedding is associated with a contraction of the length of the formation zone at $y/D = 0$, Fig. 4b). In the plane of symmetry, $z/D = 0$, the correlations show a particular organization with an

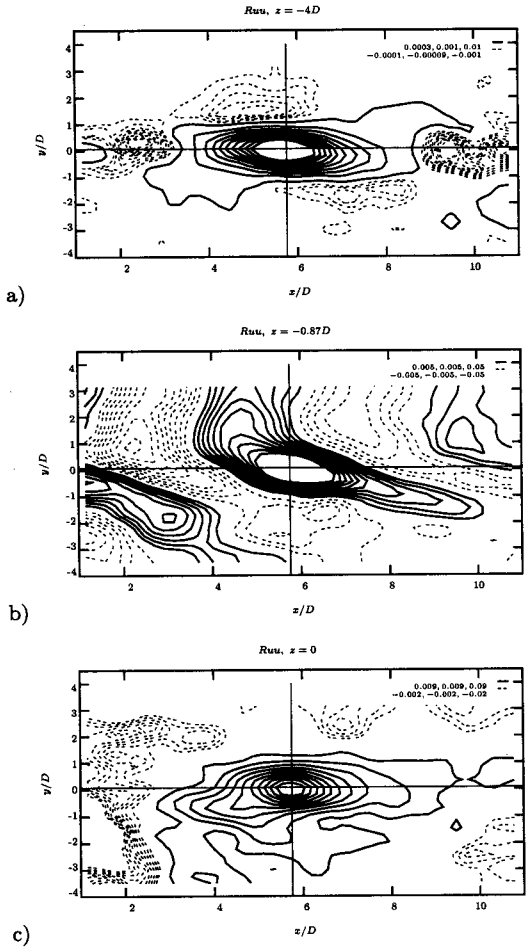

Figure 5: Isocontour of correlation $\frac{\overline{u(x_a,y_a)u(x,y)}}{(U_a-U_b)^2}$, positive level – and negative level ... : a) $z/D = -4$ b) $z/D = -0.87$ c) $z/D = 0$

integral length scale ($\Lambda_x \sim 12D$) which is twice that found in the mixing layer area, Fig. 5c. This length scale can be associated to a frequency of the order of $f \simeq 150Hz$. This observation, associated with a global movement toward the high velocity side, found from the mean velocity field, highlights the peculiar organization of the flow in this plane.

In order to develop a better understanding of this specific organization, a Low Order Dynamical System (LODS) approach is implemented, via a POD-Galerkin projection, in this plane.

POD Eigenvalues and Eigenvectors

In order to extract the POD eigenvectors from the symmetric plane, $z/D = 0$, a slice POD was applied, where only correlations in this plane were taken into account.
This problem leads to the Fredholm integral eigenvalue problem, equation (2).

$$\sum_{j=1}^{2} \int_{\Omega} R_{ij}(\mathbf{x},\mathbf{x}')\mathbf{\Phi_j^{(n)}}(\mathbf{x}')\,\mathbf{dX}' = \lambda^{(n)}\mathbf{\Phi_i^{(n)}}(\mathbf{x}) \qquad (2)$$

Practically we solve this problem by considering the following matrix diagonalization problem,

$$\mathbf{A\Phi} = \mathbf{\Lambda\Phi}, \qquad (3)$$

and by finding the eigenvectors and eigenvalues of a symmetrical definite-positive matrix A, where $\mathbf{A}$ is a discrete representation of the two points velocity cross-correlation tensor. The correlation tensor is obtained from block ensemble average, according to stationary and ergodicity hypothesis, $R_{ij}(\mathbf{x},\mathbf{x}') =< u_i(\mathbf{x})u_j(\mathbf{x}') >$, where $\mathbf{x}=(x,y,z)$. According to the Hilbert-Schmidt theory, solutions of equation(2) can be expressed as

$$u_i(\mathbf{x},t) = \sum_n a^{(n)}(t)\Phi_i^{(n)}(\mathbf{x}) \qquad (4)$$

with projection coefficients,

$$a^{(n)} = \int_{\mathcal{D}} u_i(\mathbf{x},t)\Phi_i(\mathbf{x},t)d\mathbf{x}. \qquad (5)$$

In our case, even if the eigenvectors can be obtained, this projection is not possible in a 3D2C POD, because only partial measurements (two slices from the full domain) are performed at the same time.

The size of the discrete correlation tensor, $\mathbf{A}$ to be solved (Eq.3) is equal to $N = N_x \times N_y \times n_c = 45 \times 27 \times 2 = 2430$ which is the number of discrete eigenvalues to be calculated. As shown in figure 6, 12% of the total number of modes are enough to retrieve 99% of the total energy , $E = \sum^N \lambda_i$. In figure 6, the number of modes is related to the total number of POD modes calculated, N. This figure shows a very rapid convergence of the POD modes but due to the huge size of the POD problem solved 12% still correspond to 269 modes. As a compromise between the need to reduce the size of the system to be solved and the concern for keeping a significant part of total energy, we retained the 15 first modes which contained 43.5% of the total energy for the POD-Galerkin projection.

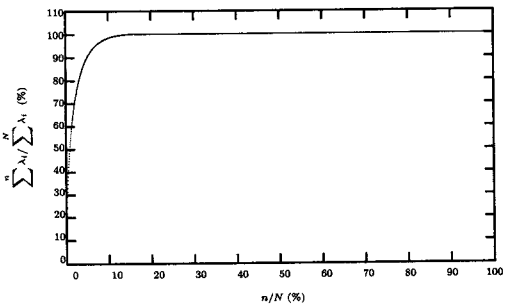

Figure 6: Convergence of the eigenvalue extracted from a 2D2C POD at $z/D = 0$

Corresponding eigenvectors were calculated for the eigenmodes. The first and second POD modes, shown in figure 7(a) and (b), show movement of large scales from the high velocity side to the low velocity side of the shear layer. For higher modes, above mode 4, smaller scales appear to be superimposed on the large scales. As an example the mode 15 shown in figure 7(c).

POD-GALERKIN

It appears that the first $n_{gal} = 15$ modes are energetically significant and were retained in the truncation of the system. Then, a Galerkin projection is performed on the fluctuating vorticity formulation of the Naviers-Stokes equations to develop a LODE.

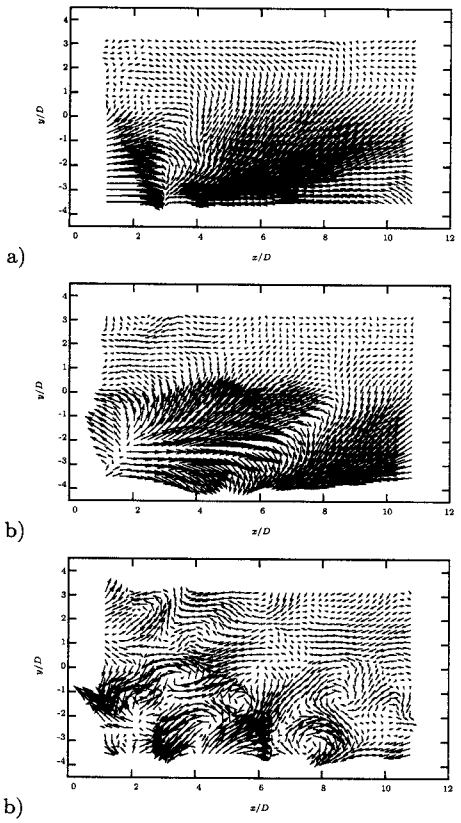

Figure 7: Eigenvector fields from a 2D2C POD at $z/D = 0$ a) mode 1 b) mode 2 c) and mode 15

Formulation

The fluctuating velocity field $\mathbf{u}$ is expressed as a linear combination of the POD modes (4), and a decomposition for the fluctuating vorticity field $\mathbf{\Omega}$ is expressed as

$$\Omega_i(x,y,t) = \sum_{n=1}^{n_{gal}} a^{(n)}(t)\Psi_i^{(n)}(x,y) \qquad (6)$$

where $\Psi_i^{(n)}(x,y) = rot(\Phi_i^{(n)}(x,y))$. The Galerkin projection on the fluctuating vorticity formulation of the Naviers Stokes equations gives

$$\int \Psi \cdot \left(\frac{\partial \mathbf{\Omega}}{\partial t} + \mathbf{u}\cdot\nabla\mathbf{\Omega} - \mathbf{\Omega}\cdot\nabla\mathbf{u} + \frac{1}{Re}\nabla^2\mathbf{\Omega} \right) d\mathbf{x} = 0 \qquad (7)$$

The equations were developed in the plane of symmetry, $z/D = 0$. A spanwise contribution is added as given by the continuity equation[1], $\Phi_{w,z} = -\Phi_{u,x} - \Phi_{v,y}$ and $w_{,z} = -u_{,x} - v_{,y}$. We note that this formulation is equivalent to considering odd (Φ_w) and even (Φ_u, Φ_v) eigenvectors components with respect to the plane of symmetry. To model the contribution of Φ_{v,x,z^2} and Φ_{u,y,z^2} we used an assumption of local isotropy,

$$\Phi_{v,x,z^2} = 2\Phi_{v,x,y^2} \qquad (8)$$

$$\Phi_{u,y,z^2} = 2\Phi_{v,y,x^2} \qquad (9)$$

This approach leads to the following dynamical system, for $n = 1, n_{gal}$, where n_{gal} is the number of modes included in the reconstruction.

$$\frac{da^{(n)}}{dt} = \sum_{m=1}^{n_{gal}} \left[\mathbf{L} + \frac{1}{Re}(1+\alpha)\mathbf{L}' \right] a^{(m)} + \sum_{m,k=1}^{n_{gal}} \mathbf{Q}\left(a^{(m)}a^{(k)} - \overline{a^{(m)}a^{(k)}} \right) \qquad (10)$$

$\mathbf{L}$,$\mathbf{L}'$ and $\mathbf{Q}$ are linear and quadratic coefficients computed employing second-order finite differences. The coefficient α accounts for truncation by modeling the energy transfer between the retained modes and the truncated modes. The mean velocity profile from experiments was used to calculate coefficients in equations (10). The third component of the vorticity was calculated from the following $\Omega_z = v_{,x} - u_{,y}$. To model mean velocity-fluctuation interaction $\overline{a^{(m)}a^{(k)}}$, we assume that the coefficients $a(t)$ satisfy the POD decomposition and hence $\overline{a^{(m)}a^{(k)}} = \lambda^{(m)}\delta_{mk}$.

Results and discussions

Equation (10) was solved using a Fourth order Runge-Kutta integration. Several tests have been conducted on the variation of the number α. The level of truncation, 15 equations from the original 2430, leads to a great loss of dissipation and a trivial solution is found for $\alpha = 30$. Below a critical level of $\alpha_c \sim 20$ the system diverges. The dynamical system behavior shows stable limit cycles in the range $20 < \alpha < 30$. Therefore α, in the context of dynamical systems, can be considered as a bifurcation parameter. Stable limit cycles are obtained for $tU_m/D = 3500$ time steps which corresponds to 900 vortex shedding periods, based on the high velocity side. A time history of the critical limit cycle, $\alpha \simeq 20$, is shown figure (8).

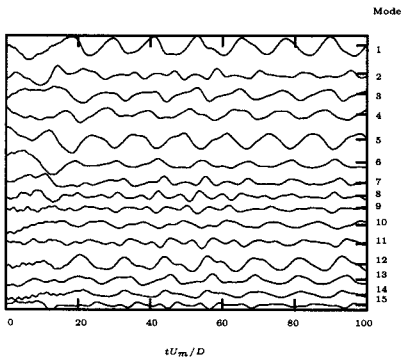

Figure 8: Signal $a^{(n)}(t)$ from the dynamic system of 15 equations and $\alpha \sim 20$

A spectral density analysis of the dynamical system signals exhibits two main frequencies whose peaks are dominant for all modes under consideration. One frequency, at 155Hz, appears to be associated with the integral length scale analysis at $z/D = 0$, figure 5c). The second frequency, at around twice this value (316Hz), is related to the frequency ($f_{pa} \sim 300$Hz) of the mixing layer. The relation between the two frequencies can be observed in the corresponding phase portrait, constructed by cross-plotting the coefficient of the third mode versus the first mode (Fig. 9a) and the eleventh mode versus the first mode (Fig. 9b) for example.

Furthermore, visualization of the reconstructed fluctuating velocity field (Eq. 4), highlights a pulsed injection of fluid towards high velocity side at $\sim$ 150Hz which is consistent with previous results (Heitz, 1999).

[1] We note $f_{u,x} = \frac{\partial f_u}{\partial x}$, $f_{u,x,z^2} = \frac{\partial^3 f_u}{\partial x \partial z^2}$

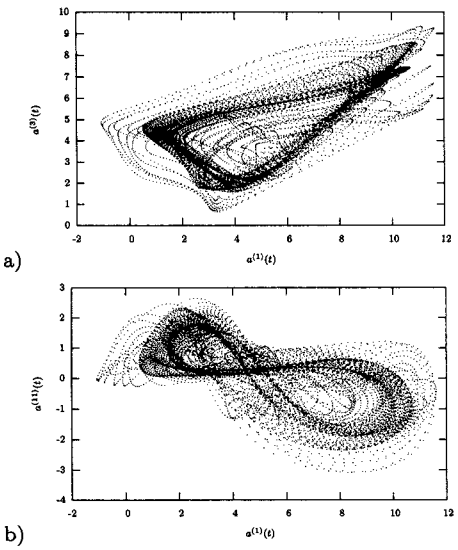

Figure 9: Phase space : a) $a^{(3)}(t)$ versus $a^{(1)}(t)$ b) $a^{(11)}$ versus $a^{(1)}$

CONCLUSIONS

The interaction between the mixing layer and a cylinder wake was first analyzed through the mean velocity field which revealed a decomposition of the flow into distinct regions. It appears that a local injection of fluid from the low to high velocity side of the mixing layer is an important feature of the flow. The analysis of two point correlations in specific areas provides evidence of characteristic length scales and frequencies for the different regions depending on whether the flow was dominated by mixing layer, the wake, or the interaction of the two. Results where consistent with previous studies which showed oblique shedding. Slice POD was applied in the symmetry plane of the flow, $z/D = 0$. Eigenvalues and eigenvectors were calculated and it was found that it was possible to keep only then first 15 POD modes to construct a dynamical system accounting for the main characteristics of the flow. The LODE showed the same spectral characteristics as the experiments, namely the appearance of the two dominant frequencies. The fluctuating velocities reconstructed from the dynamical system clearly showed a periodic fluid injection from the low to high speed regions of the flow with a frequency and direction consistent with previous experimental observations.

REFERENCES

ALFONSI, G., RESTANO, C. & PRIMAVERA, L., 2003, "coherent structures of the flow around a surface-mounted cubic obstacle in turbulent channel flow", *Journal of Wind Ingineering and Industrial Aerodynamics*, Vol. 91, pp. 495–511.

AUBRY, N., HOLMES, P., LUMLEY, J. & STONE, E., 1988, "the dynamics of coherent structures in the wall region of a turbulent boundary layer", *J. Fluid Mech.*, Vol. 192, pp. 115–173.

BEARMAN, P. W., 1998, "developments in the understanding of bluff body flows", *JSME International Journal*, Vol. 41 (1), series B.

BERNERO, S. & FIEDLER, H. E., 2000, "application of particule image velocymetry and proper orthogonal decomposition to the study of a jet in a counterflow". *Exp. in fluids*, Vol. Suppl, pp. S274–S281.

BRAUD, C., HEITZ, D., BRAUD, P., ARROYO, G. & DELVILLE, J., 2002, "investigation of plane mixing layer - wake interaction by means of two 2D PIV planes and of POD", In *International Symposium on applications of laser techniques to fluid mechanics, 11 th* session 32.

DELVILLE, J., UKEILEY, L., CORDIER, L., BONNET, J. & GLAUSER, M., 1999, "examination of large-scale structures in a turbulent plane mixing layer. part 1. proper orthogonal decomposition", *J. Fluid Mech.* Vol. 391, pp. 91–122.

HEITZ, D., 1999, Etude expérimentale du sillage d'un barreau cylindrique se développant dans une couche de mélange plane turbulente. PhD thesis, Poitiers University.

HOLMES, P., LUMLEY, J. & BERKOOZ, G. 1996 *Turbulence, Coherent Structures, Dynamical Systems and Symmetry*. Cambridge University Press.

HOLMES, P., LUMLEY, J., BERKOOZ, G., MATTINGLY, J. & WITTENBERG, R., 1997, "low dimensional models of coherent structures in turbulence", *Physics Reports*, Vol. 287, pp. 337–384.

KAEHLER, C., 2000, "multiple plane stereo piv - recording and evaluation methods", In *EUROMECH 411, Appl. of PIV to tubulence measurements*. University of Rouen, France.

LUMLEY, J., 1967, "the structure of inhomogeneous turbulent flows". In *Atmospheric Turbulence and Radio Wave Propagation*, (ed. A. Yaglom & V. Tatarski),pp. 166–178.

MA, X. & KARNIADAKIS, G., 2002, "a low-dimensional model for simulating three-dimensional cylinder flow", *J. Fluid Mech.*, Vol. 458, pp. 181–190.

MANHART, M., 1998, "vortex shedding from a hemisphere in a turbulent boundary layer", *Theoret. Compt. Fluid Dynamics*, Vol. 12, pp. 1–28.

RUELLE, D. & TAKENS, F., 1971, "on the nature of turbulence", *Communs. Math. Phys.*, Vol. 82, pp. 137.

SIROVICH, L., 1987, "turbulence and the dynamics of coherent structures.part 1 :coherent structures", *Quarterly of Applied Mathematics XLV*, Vol. 3, pp. 561–571.

STEPHEN, A. V., MOROZ, I. M. & READ, P. L., 1999, "pod analysis of baroclinic wave flows in the thermally-driven, rotating annulus experiment", *Phys. Chem. Earth(B)*, Vol. 24 (5), pp. 449–453.

UKEILEY, L., CORDIER, L., MANCEAU, R., DELVILLE, J. & BONNET, J., 2001, "examination of large-scale structure in turbulent plane mixing layer. part 2. dynamical systems model", *J. Fluid Mech.*, Vol. 441, pp. 67–108.

WILLIAMSON, C. H. K., 1996, "vortex dynamics in the cylinder wake", *Ann. Rev. Fluid Mech.*, Vol. 28, pp. 477–539.